Near-field optical spectroscopy of localized excitons in strained CdSe quantum dots

F. Flack and N. Samarth
Department of Physics, The Pennsylvania State University, University Park, Pennsylvania 16802

V. Nikitin, P. A. Crowell, J. Shi, J. Levy, and D. D. Awschalom
Department of Physics, University of California, Santa Barbara, California 93106
(Received 5 September 1996)

Control of the growth dynamics during the epitaxy of coherently strained ZnSe/CdSe quantum structures results in a varied interfacial texture that broadly defines two qualitatively different regimes for exciton localization. An island growth mode produces quantum dot regions in which the lateral confinement of excitons is directly revealed through the observation of resolution-limited (full width at half maximum of <0.8 meV) emission peaks in near-field photoluminescence spectra. By contrast, layer-by-layer growth produces potential fluctuations at length scales small compared to the exciton diameter, so that the localization of excitons is driven by a random interfacial potential with a smooth density of states. [S0163-1829(96)50948-3]

The past few decades have witnessed rapid advances in the fabrication of semiconductor nanostructures. Zero-dimensional (0D) semiconductor quantum dots in particular continue to attract substantial attention both because of unresolved issues regarding fundamental limitations on their intrinsic quantum efficiency (the ''phonon-bottleneck'' problem)[1] and because of recent successes with *in situ* fabrication of defectfree, self-assembled ensembles of strained III-V quantum dot structures with surprisingly high quantum efficiencies and relatively narrow size distributions.[2] We discuss here the first *direct* observation[3] of 0D exciton confinement in *wide-gap* II-VI quantum structures formed during the strained layer epitaxy of (cubic) CdSe ($E_g=1.75$ eV) on ZnSe ($E_g=2.8$ eV) with a lattice mismatch $\Delta a/a\sim 0.07$.[4]

By varying the dynamical growth conditions during the epitaxy of CdSe, we broadly define two qualitatively different regimes of interfacial texture that affect the nature of exciton localization. Stranski-Krastonow (SK) island growth yields quantum dot regions in which excitons are laterally confined with an associated 0D density of states that is consistent with resolution-limited spectral structure in photoluminescence (PL) spectra taken using a near-field scanning optical microscope (NSOM). By contrast, layer-by-layer growth produces ''pseudosmooth'' quantum wells with a spatially varying quasi-2D confining potential in which exciton localization may occur in the disorder-induced low-energy tail of a smooth density of states.

As a result of the deep confining potentials for electrons and holes in these ZnSe/CdSe quantum structures, both quantum-well and quantum-dot samples exhibit efficient PL up to room temperature and hence are worth exploring as media for the active region in visible light-emitting diodes. Further, the observation of 0D states in II-VI nanostructures opens up exciting possibilities for studying static and dynamic *spin-dependent phenomena* in ''quantum spin dots'' by the incorporation of magnetic ions into II-VI nanostructures.[5] Finally, it is pertinent to point out that these samples are characterized by length scales for exciton localization that are quite different from those encountered in earlier studies of islandlike defects in III-V quantum wells[6] (where the lateral extent of the confining potential is comparable to or much larger than the exciton diameter) and self-assembled III-V quantum dots[2] (where 0D confinement occurs in islands with a larger height-diameter ratio). This difference is attributed to lower surface mobilities and large interdiffusion in these II-VI heterostructures.

Molecular-beam epitaxy (MBE) is used to deposit coherently strained epitaxial layers of CdSe sandwiched between a 700-nm buffer layer of ZnSe on (100) GaAs and a 100-nm ZnSe cap layer. *In situ* reflection high-energy electron diffraction (RHEED) studies characterize the growth rate and the critical thickness t_c at which a transition occurs from layer-by-layer epitaxy to SK island growth. Two distinct classes of CdSe quantum structures are investigated: (a) quantum-''well'' structures formed during layer-by-layer epitaxy at a substrate temperature $T_s\sim 300$ °C and in which the quantum-well thickness does not exceed t_c and (b) quantum-''dot'' structures formed by depositing layers of CdSe with thicknesses barely greater than t_c at higher substrate temperatures (400 °C$<T_s<$450 °C), while monitoring the transition from layer-by-layer to SK growth.

For $T_s\sim 300$ °C, pseudosmooth CdSe layers (i.e., a disordered 2D surface characterized by well-defined streaks in the RHEED pattern) can be deposited up to a critical thickness $t_c\sim 3$ ML using a growth of rate ~ 0.05 ML/s. This regime of layer-by-layer growth is accompanied by the observation of clear RHEED oscillations. Once the critical thickness is exceeded, a distinct roughening transition occurs, indicated by a marked drop in the intensity of the specular reflection.[7] At these lower substrate temperatures, the roughening transition is also accompanied by a gradual broadening of the RHEED streaks and a relaxation of the strained CdSe lattice, presumably through the formation of misfit dislocations. This scenario is supported by a dramatic drop in PL efficiency for samples containing a CdSe layer thickness larger than t_c, signaling the formation of nonradiative centers through dislocation formation.

For $T_s>400$ °C, when the critical thickness is exceeded, the lattice minimizes strain energy by the formation of coherently strained islands rather than by the formation of dis-

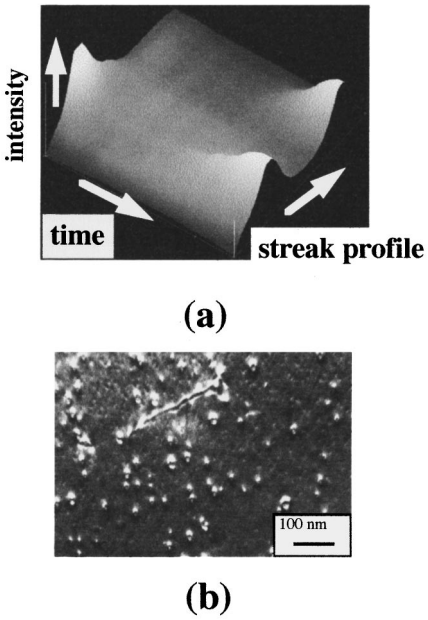

FIG. 1. (a) Time variation of the intensity profile of the zero-order RHEED streak during the growth of CdSe at 425 °C, showing the transition from a ''smooth'' 2D surface to a rough 3D transmission pattern. Simultaneous measurements of the intensity of the specular beam show a sudden damping on RHEED oscillations at the 2D-3D transition. (b) Plan-view TEM image of a ZnSe/CdSe quantum structure showing the presence of CdSe islands formed by exploiting the transition to 3D growth. The island density is $\sim 200/\mu m^2$.

locations; this onset of SK growth is indicated by the transformation of the RHEED streaks into well-defined spots [Fig. 1(a)]. Plan-view transmission electron microscopy (TEM) shows the presence of islands with diameters ranging between 10 to 20 nm [Fig. 1(b)]. While the heights of the islands cannot be directly assessed without additional cross-sectional TEM measurements, we will later present estimates obtained from PL spectra. In these strained islands, the PL efficiency does *not* show a marked drop when the critical thickness t_c is exceeded, strongly suggesting that strain relief through defect formation has been suppressed. We further note that RHEED studies over the substrate temperature range $300\ °C < T_s < 450\ °C$ indicate that t_c does not show much variation with T_s and remains roughly in the range 2–3 ML. This is at variance with both experimental studies and simulations of other strained systems that show a marked decrease in t_c at higher substrate temperatures as a result of the enhanced surface diffusion length.[8] The fundamental difference in growth kinetics observed here may be attributed to enhanced interdiffusion with increasing T_s: this provides a channel for strain relief that competes with energy minimization through islanding. The acute onset of interdiffusion at ZnSe/CdSe interfaces for temperatures in excess of 450 °C is unequivocally demonstrated by the observation of pronounced blueshifts in the PL spectra of ZnSe/CdSe quantum wells subject to rapid thermal annealing.[9] Further evidence for interdiffusion in this system is also reported in recent RHEED–high-resolution TEM studies.[10]

The varying interfacial texture brought about by the two classes of dynamical growth modes described above has a direct effect on exciton localization in these CdSe quantum structures. As shown earlier, this is reflected in a clear redshift in the PL of quantum-dot samples compared with quantum-well samples containing the same amount of deposited CdSe.[7] Deeper physical insight into the differences between exciton localization in these two regimes is obtained through PL spectroscopy with high spatial resolution (~100 nm) carried out using both a low-temperature NSOM (the details of which are described elsewhere[11]) and conventional far-field PL on masked samples that have circular window areas with diameters ranging down to 100 nm.

NSOM PL spectra and images of the CdSe quantum structures are obtained by exciting the samples with the 442-nm line of a He-Cd laser guided through the NSOM optical fiber tip and detecting the emitted PL in the far field on the opposite side of the sample using a charge-coupled device array; the GaAs substrate is etched away for such measurements. The effective sample area being probed in this scheme is then at least the size of the excitation region (~100 nm) but could be larger due to exciton diffusion. Figure 2(a) shows the difference between the NSOM PL spectrum (at 5 K) in an island growth sample when the excitation source is brought from the far field into the near field regime. The smooth, inhomogeneously broadened lineshape of the far field PL spectrum evolves into a spectrum characterized by sharp, resolution-limited (0.8 meV) reproducible spectral features. These sharp features are attributed to the recombination of ground-state excitons laterally confined to quantum-dot regions; the near-field PL spectrum is a convolution of the δ-function density of states of each individual quantum-dot region and an envelope determined by the statistical distribution of quantum-dot shapes and sizes. Note that—in strong contrast—the near-field PL spectrum of a layered growth quantum-well sample does not show any such sharp structure (Fig. 3) and is qualitatively identical to the far-field PL spectrum.[7]

The NSOM PL technique also allows us to construct a PL image at any particular energy by collecting spectra as the NSOM tip is rastered over the sample. Figures 2(b) and 2(c) show two such images at detection energies of 2.1875 and 2.2375 eV, respectively. As the detection energy is increased or decreased by more than 2 meV, the bright features disappear and new ones appear at different locations on the sample. The bright areas extend over larger regions (~0.4 μm) than our spatial resolution or the sizes of the dots observed in TEM measurements. This discrepancy is attributed to the diffusion of excitons from the approximately 100-nm photoexcitation region into nearby quantum-dot regions, so that our far-field detection scheme actually measures a convolution of the local energy landscape and the exciton diffusion profile.

The δ-function nature of the density of states in the quantum-dot samples is confirmed through high spectral resolution far-field PL studies by using electron-beam lithography to define circular windows with diameters ranging down to 100 nm in metallically coated samples. While such spectroscopy does not have the spatial PL imaging capability of the NSOM technique, carriers are excited and luminescence is collected from the same small area, thus avoiding the issues of diffusion discussed above. Figure 4 shows PL spectra obtained in this manner, clearly demonstrating the

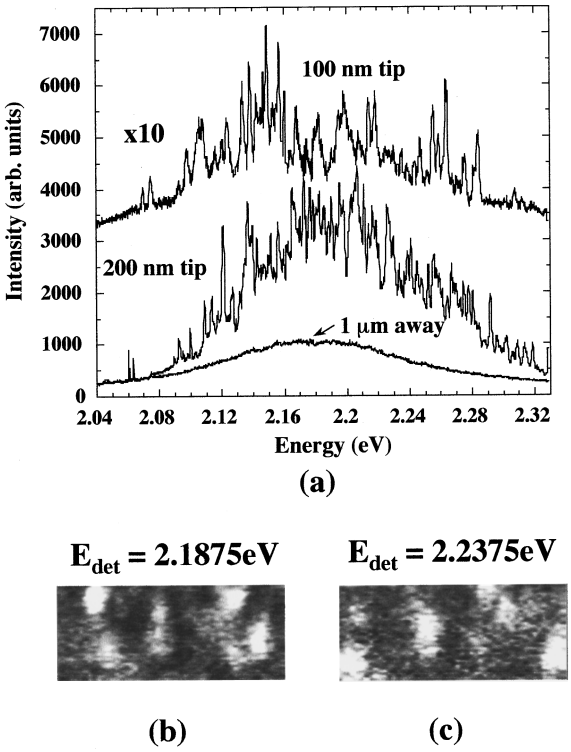

FIG. 2. (a) Low-temperature (5 K) NSOM PL spectra from an island growth sample containing a total deposition of 3 ML of CdSe. The lower spectra are shown for two different distances between the 200-nm diameter NSOM tip and the sample, marking the transition from the far-field to the near-field regime. The uppermost spectrum shows a very high spatial resolution NSOM scan from a different region of the same sample with a tip of 100-nm diameter. (b) NSOM PL images from a 2 μm$\times$4 μm sample region taken at two fixed energies of 2.1875 and 2.2375 eV using a tip of 100 nm diameter.

resolution-limited nature of the PL emission from individual quantum-dot regions. The presence of both sharp emission lines and a broad background in the quantum dot PL indicates a fairly dense, nonuniform distribution of quantum-dot regions. In addition, the temperature-dependent spectra in Fig. 4 show that the sharp spectral features gradually merge into broader lines at higher temperatures, indicating the thermal activation of excitons out of the quantum-dot regions.

The detailed nature of the quantum-dot regions is difficult to assess at this stage without high-resolution cross-sectional

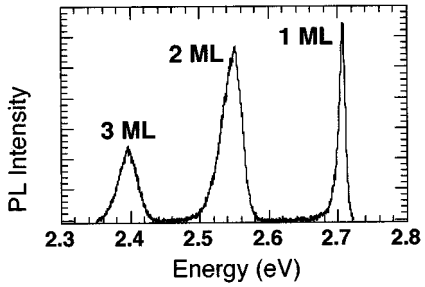

FIG. 3. Low-temperature (5 K) NSOM PL spectrum of a sample containing 3 isolated quantum well-regions of 1, 2, and 3 ML of CdSe grown under layer-by-layer epitaxy conditions $T_s \sim 300$ °C.

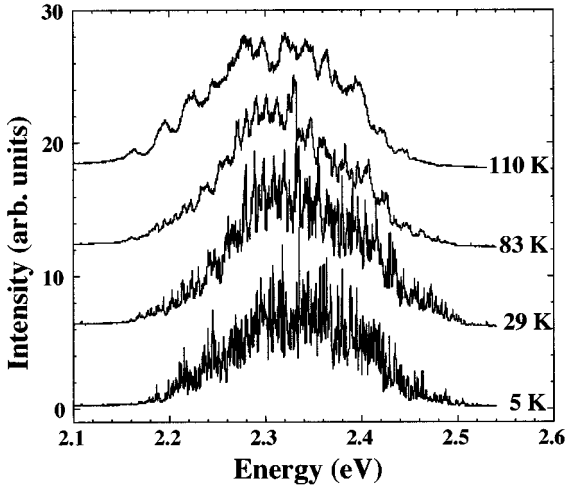

FIG. 4. Temperature-dependent far-field PL spectra taken from a 250-nm diameter circular region of a patterned quantum-dot sample.

TEM, particularly given the complex interface and strain profile that results from the combined effects of interdiffusion and islanding. (It has recently been suggested that such interface disorder complicates the interpretation of optical data even in the better characterized III-V quantum-dot samples.[12]) However, it is instructive to obtain a rough estimate of the relevant length and energy scales characterizing the quantum-dot regions using a simple one-particle calculation that models the quantum-dot regions by an ensemble of uniformly strained CdSe boxes of size $L \times L \times h$, with a Gaussian distribution for the lateral dimension L. Assuming the PL to arise from the recombination of confined ground-state electron–heavy-hole excitons, we find that the inclusion of single monolayer variations in the height h leads to substantially larger widths ($\sim$300 meV) for the inhomogeneous PL envelope than those observed experimentally ($\sim$100 meV), strongly suggesting that the variation in emission energies arises from fluctuations in the lateral island size and potential fluctuations due to interdiffusion. Comparisons between the model calculations and experiment suggest that the mean height to lateral size aspect ratios of the CdSe quantum-dot regions are small compared to those found in III-V self-assembled nanostructures. For instance, the PL spectrum of quantum-dot samples fabricated by depositing 2–3 ML of CdSe would imply a mean island height of at most 5 ML ($\sim$1.5 nm) and a mean island diameter of $\sim$10 nm.

Finally, we briefly address the NSOM PL spectrum of the quantum-well sample described earlier, which does not show any sharp line structure. The inhomogeneous PL linewidths in such quantum-well samples arise from random interface potential fluctuations that occur at a length scale *small* compared to the exciton diameter ($\sim$9 nm for CdSe). In contrast to the quantum-dot samples, the density of states here is not discrete and excitons undergo localization in the disorder-induced low-energy tail of the density of states.[13] This picture is consistent with large observed Stokes shifts ($\sim$30 meV) between PL and absorption spectra in these quantum-well samples.[7] Such a regime for interface roughness is unlike that usually encountered in the III-V semiconductors

where interface fluctuations occur either at length scales comparable to the exciton diameter or much larger than the exciton diameter. The random potential fluctuations can arise either because of monolayer fluctuations or the interdiffusion of the ZnSe and CdSe regions, with the exciton wave function then sampling a statistical average of the fluctuating potential. It is easily estimated that monolayer fluctuations over distances comparable to the exciton diameter would lead to substantially larger linewidths (~300 meV) than those observed (~30–50 meV). Finally, we note that interdiffusion at very modest scales can easily account for the observed linewidth because the energy gap of the alloy $Zn_{1-x}Cd_xSe$ varies rapidly with composition (roughly 10 meV for a change of $\Delta x = 0.01$).

In summary, the careful exploitation of a 3D growth mode yields efficient PL from quantum-dot regions created by coherently strained CdSe islands. The associated discrete density of states is directly revealed through near-field PL measurements. The smaller surface diffusion lengths in these II-VI materials coupled with a higher degree of interdiffusion yield ensembles of islands with a smaller average height and a larger size dispersion than in the III-V semiconductors. By contrast, in quantum-well structures grown using layer-by-layer epitaxy, recombining excitons are efficiently localized by disordered potential fluctuations over length scales small compared to the exciton diameter.

This work was supported by grants from the Office of Naval Research (ONR N00014-94-1-0297 and -0225), the Air Force Office of Scientific Research (F49620-96-1-0118), the National Science Foundation (DMR-92-07567 and -95-00460), and the NSF Science and Technology Center for Quantized Electronic Structures (DMR 91-20007).

Note added in proof. Direct signatures of OD excitons have also been recently observed in islandlike defects in strained (Zn,Cd)Se quantum wells [M. Lowsch *et al.*, Phys. Rev. B **54**, R11074 (1996)].

[1] U. Bockelmann and G. Bastard, Phys. Rev. B **42**, 8947 (1990); H. Benisty, C. Sottomayor-Torres, and C. Weisbuch, *ibid.* **44**, 10 945 (1991).

[2] J. Y. Marzin *et al.*, Phys. Rev. Lett. **73**, 716 (1994); R. Leon *et al.*, Science **267**, 1966 (1995); M. Grundmann *et al.*, Phys. Rev. Lett. **74**, 4043 (1995).

[3] We note that recent PL studies of other wide-gap II-VI heterostructures containing submonolayers of ZnSe have indirectly suggested the presence of quantum dot states—see, for instance, T. Wu, K. Arai, and T. Yao, Phys. Rev. B **53**, R10 485 (1996).

[4] N. Samarth *et al.*, Appl. Phys. Lett. **54**, 2680 (1989); H. Zajicek *et al.*, *ibid.* **62**, 717 (1993); Z. Zhu *et al.*, *ibid.* **63**, 1678 (1993).

[5] V. Nikitin *et al.*, in *Proceedings of the International Conference on the Physics of Semiconductors* (World Scientific Press, Singapore, 1996), Vol. 2, p. 1441.

[6] H. F. Hess *et al.*, Science **264**, 1740 (1994); K. Brunner *et al.*, Phys. Rev. Lett. **73**, 1138 (1994).

[7] F. Flack *et al.*, in *Optoelectronic Materials: Ordering, Composition Modulation and Self-Assembled Structures*, edited by E. D. Jones, A. Mascarhenhas, and P. M. Petroff, MRS Symposia Proceedings No. 417 (Materials Research Society, Pittsburgh, 1996), p. 169.

[8] B. G. Orr, D. Kessler, C. W. Snyder, and L. Sander, Europhys. Lett. **19**, 33 (1992); C. W. Snyder, B. G. Orr, D. Kessler, and L. Sander, Phys. Rev. Lett. **66**, 3032 (1991).

[9] H. Hennessey and N. Samarth (unpublished).

[10] A. Rosenauer *et al.*, J. Cryst. Growth **152**, 42 (1995).

[11] J. Levy *et al.*, Phys. Rev. Lett. **76**, 1948 (1996); J. Levy *et al.*, J. Appl. Phys. **79**, 6095 (1996).

[12] E. V. Tsiper, Phys. Rev. B **54**, 1959 (1996).

[13] E. Cohen and M. D. Sturge, Phys. Rev. B **25**, 3828 (1982).